Journal of Alloys and Compounds 509 (2011) 9111–9115

Contents lists available at ScienceDirect

Journal of Alloys and Compounds

journal homepage: www.elsevier.com/locate/jallcom

Enhanced photoluminescence of $GdPO_4$:Tb^{3+} under VUV excitation by controlling ZnO content and annealing temperature

K. Park*, M.H. Heo

Faculty of Nanotechnology and Advanced Materials Engineering, Sejong University, Seoul 143-747, Republic of Korea

ARTICLE INFO

Article history:
Received 17 February 2011
Received in revised form 14 June 2011
Accepted 15 June 2011
Available online 18 July 2011

Keywords:
Photoluminescence
Annealing
Ultrasonic spray pyrolysis
Phosphors
Powder
$GdPO_4$:Tb^3

ABSTRACT

High-quality Zn-free and added $GdPO_4$:Tb^3 green phosphors, i.e., fine size as well as smooth and spherical morphologies, were synthesized by ultrasonic spray pyrolysis. The influence of Zn^{2+} content and annealing temperature on the photoluminescence properties of the $GdPO_4$:Tb^3 phosphors annealed at 800–1100 °C was investigated. The addition of Zn^{2+} for Gd^{3+} was highly effective for improving the photoluminescence properties of $GdPO_4$:Tb^3. The Zn added $GdPO_4$:Tb^3 phosphors with Zn/Gd = 0.045/0.805 showed the strongest emission of the prepared phosphors. The emission intensity at 544 nm for the $GdPO_4$:Tb^3 phosphors with Zn/Gd = 0.045/0.805 annealed at 900 °C was 496% stronger than that at 800 °C.

1. Introduction

The remarkable narrow-band emission properties of Eu^{3+}, Tb^{3+}, Dy^{3+}, and Tm^{3+} ions have been widely utilized for the development of efficient phosphors for plasma display panels (PDPs), lamps, and light-emitting diodes [1–3]. In particular, rare-earth doped phosphates are attractive host materials for PDPs because of their excellent photoluminescence (PL) characteristics [4–9]. Finke et al. [7] synthesized potassium rare earth orthophosphates ($K_3RE(PO_4)_2$; RE = Ce^{3+}, La^{3+}, and Tb^{3+}) by a solid state reaction and studied their optical properties under ultraviolet (UV) and vacuum ultraviolet (VUV) excitations. The band gaps determined by reflection and excitation spectra ranged from 7.2 to 7.8 eV. The narrow excitation band at the VUV absorption edge originated from an excitation of $(PO_4)^{3-}$ anion molecules in the hosts. Since then, Rao and Devine [8] investigated overall PL properties of rare earth lanthanide ($LnPO_4$; Ln = Y^{3+}, La^{3+}, and Gd^{3+}) phosphate-based phosphors and their suitability in PDPs. They reported that the phosphate-based phosphors exhibited a high absorption in VUV region, compared to silicate-, borate-, and oxide-based standard PDP phosphors. The phosphors can be used in a display in conjunction with suitable absorbing filter. Green-emitting Tb^{3+}-doped Y orthophosphate YPO_4 phosphors have attracted considerable attention as a promising green emitting phosphor candidate. Di et al. [9] prepared YPO_4:Tb^{3+} phosphors by two different methods, i.e., conventional solid-state reaction route and solution-based co-precipitation route. The solution-based co-precipitation assisted YPO_4:Tb^{3+} phosphor powders showed high quality, i.e., spherical shape, narrow size distribution, and homogeneous composition. The YPO_4:Tb^{3+} phosphors under 147 nm excitation displayed better PL properties than conventional solid-state reaction assisted phosphors because of their excellent powder characteristics.

Yang et al. [10,11] studied the PL properties of $LaPO_4$ phosphate-based phosphors synthesized by both hydrothermal and solvothermal methods. $LaPO_4$, $LaPO_4$:Ce^{3+}, and $LaPO_4$:Ce^{3+},Tb^{3+} powders with various morphologies and sizes were successfully prepared by ethylenediamine tetraacetic acid disodium salt (EDTA) assisted hydrothermal method [10]. The value of pH, the concentration of EDTA, and the doping components significantly affected the morphologies and sizes of the as-prepared powders. Upon UV excitation, $LaPO_4$:Ce^{3+} and $LaPO_4$:Ce^{3+},Tb^{3+} phosphors presented the characteristic 5d–4f emissions of Ce^{3+} and $^5D_4$–^7F_J, (J = 6–3) emissions of Tb^{3+}, respectively. In addition, luminescent $LaPO_4$:Eu^{3+}, $LaPO_4$:Ce^{3+}, and $LaPO_4$:Ce^{3+},Tb^{3+} powders were successfully synthesized using oleic acid as capping agents via a solvothermal process [11]. All the prepared $LaPO_4$-based phosphors crystallized in the monoclinic monazite-type structure. The prepared phosphors showed a narrow size distribution along with an average powder size of about 15 nm. Upon excitation by UV radiation, the $LaPO_4$:Eu^{3+} phosphors showed the characteristic $^5D_0$–$^7F_{1-3}$ emissions of Eu^{3+}, while the $LaPO_4$:Ce^{3+},Tb^{3+} showed the characteristic $^5D_4$–$^7F_{3-6}$ emissions of Tb^{3+}.

* Corresponding author. Tel.: +82 2 3408 3777; fax: +82 2 3408 3664.
E-mail address: kspark@sejong.ac.kr (K. Park).

0925-8388/$ – see front matter © 2011 Elsevier B.V. All rights reserved.
doi:10.1016/j.jallcom.2011.06.063

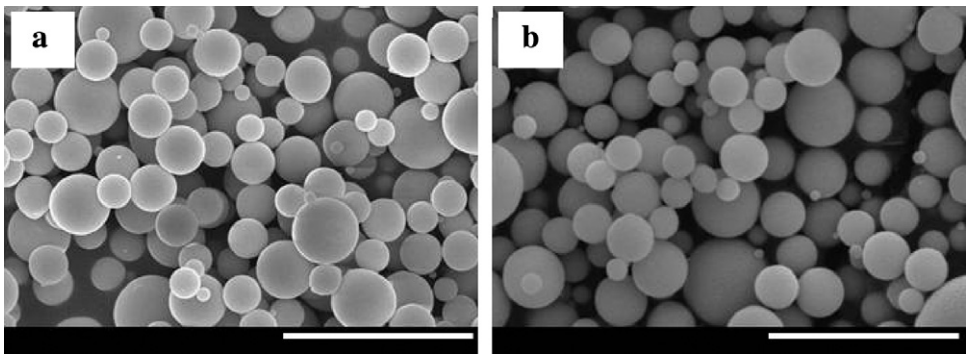

Fig. 1. SEM image of the as-synthesized Zn-added $GdPO_4$:Tb^3 powders with Zn/Gd: (a) 0.015/0.835 and (b) 0.03/0.82 (scale bar: 5 μm).

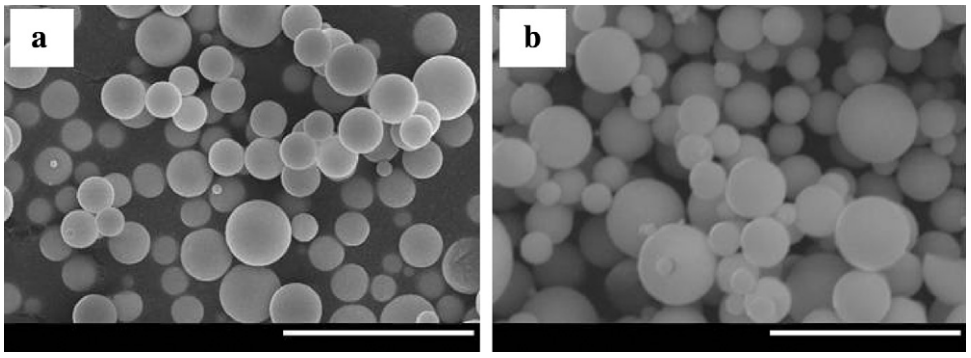

Fig. 2. SEM images of the Zn^{2+}-free $GdPO_4$:Tb^3 phosphors annealed at (a) 800 °C and (b) 1000 °C (scale bar: 5 μm).

It is known that controlling the composition and/or process, especially annealing, is a feasible route for improving PL characteristics [12,13]. Therefore, in the present work, to improve PL characteristics, we fabricated the Zn^{2+}-added $GdPO_4$:Tb^3 phosphors annealed at various temperatures (800–1100 °C) and investigated their microstructure and PL properties, depending on the Zn^{2+} contents and annealing temperature.

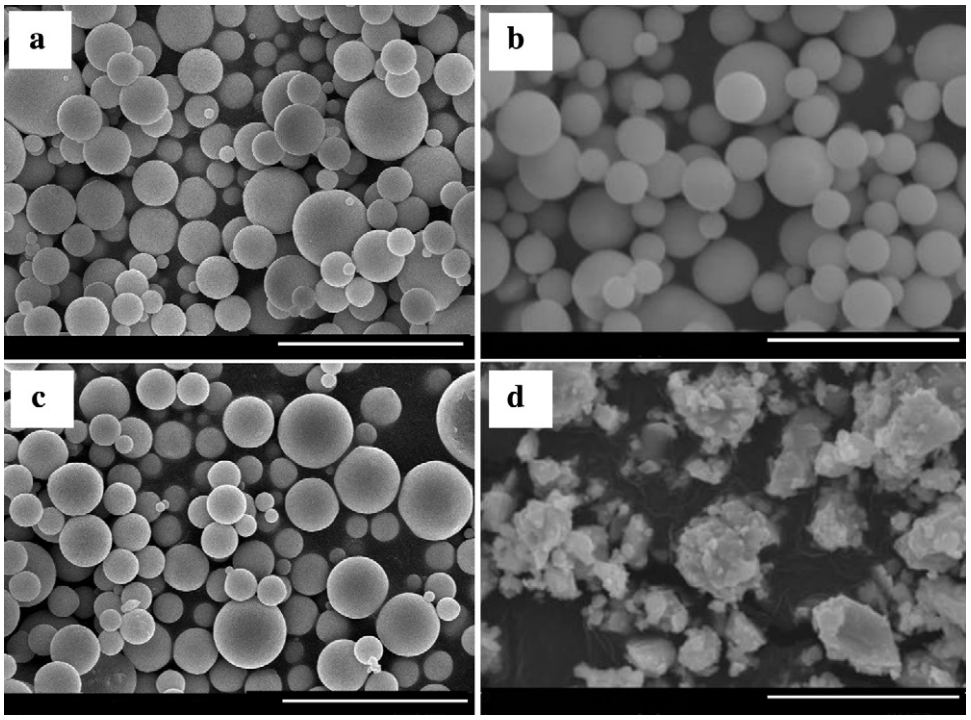

Fig. 3. SEM images of the Zn-added $GdPO_4$:Tb^3 phosphors with Zn/Gd: (a) 0.015/0.835 and (b) 0.03/0.82 annealed at 900 °C and of the Zn-added $GdPO_4$:Tb^3 phosphors with Zn/Gd: (a) 0.015/0.835 and (b) 0.03/0.82 annealed at 1000 °C (scale bar: 5 μm).

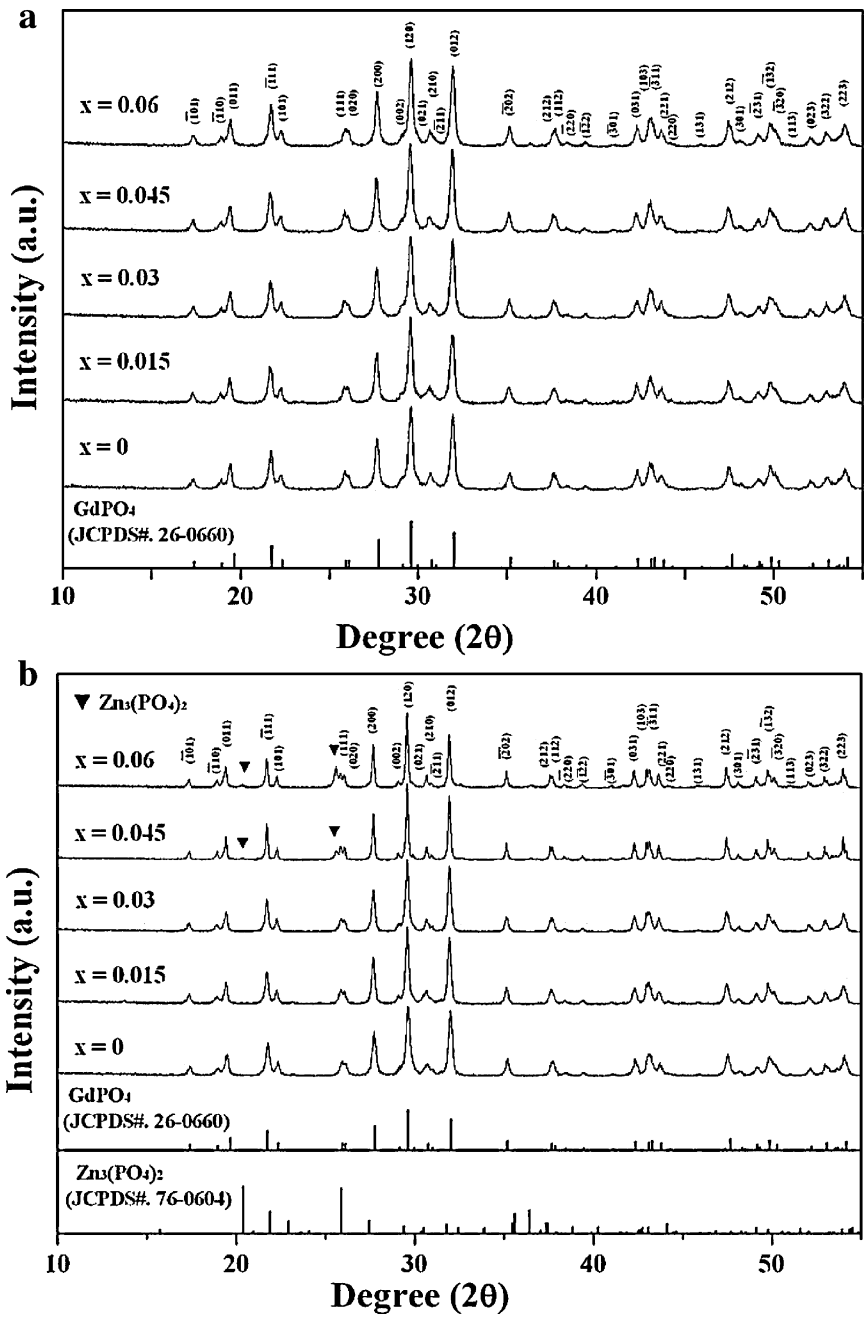

Fig. 4. XRD patterns of the $GdPO_4$:Tb^3 phosphors with various Zn^{2+} contents annealed at (a) 800 °C and (b) 900 °C.

2. Experimental

The Zn^{2+}-free and added $GdPO_4$:Tb^3 powders with Zn/Gd = 0/0.85, 0.015/0.835, 0.03/0.82, 0.045/0.805, and 0.06/0.79 (Zn + Gd = 0.85) were synthesized by ultrasonic spray pyrolysis. The system for the synthesis of the phosphors consisted of a droplet generator (1.7 MHz), a high-temperature tubular quartz reactor, and a powder collector. An ultrasonic spray generator was used to generate droplets. The length and inner diameter of the reactor were 1000 and 100 mm, respectively. The temperature of the reactor was at 1000 °C.

Gd_2O_3 (99.99%) powders were dissolved in HNO_3 and then heated at 80 °C to prepare solidified $Gd(NO_3)_3{\cdot}xH_2O$. Subsequently, Tb_2O_3 (99.9%) powders were dissolved in HCl and then heated at 80 °C to prepare solidified $TbCl_3$. $Zn(NO_3)_2{\cdot}6H_2O$ (99.9%), $Gd(NO_3)_3{\cdot}xH_2O$, and $TbCl_3$ were added to the aqueous solution containing H_3PO_4 (99.9%) and organic additives. The organic additives were composed of ethylene glycol (99.5%) and citric acid (EP). The pH of the precursor solution was controlled at 2.0 by adding HNO_3. The reaction mists formed in the ultrasonic nebulizer were transferred into the quartz reactor (1000 °C) by air (20 l/min in flow rate). The synthesized phosphor powders were annealed at 800–1100 °C for 4 h and subsequently cooled to room temperature.

A scanning electron microscope (SEM; Hitachi S4700) was used to investigate the microstructure of the synthesized and annealed Zn^{2+}-added $GdPO_4$:Tb^3 phosphors. The crystal structure of the annealed phosphors at room temperature was characterized with an X-ray diffractometer (XRD; Rigaku RINT2000). The PL properties of the phosphors at room temperature were measured with a spectrofluorophotometer (PSI) equipped with a D_2 flash lamp. The emission spectra were obtained under VUV region (147 nm).

3. Results and discussion

We synthesized high-quality Zn^{2+}-added $GdPO_4$:Tb^3 green phosphor powders, i.e., fine size as well as smooth and spherical morphologies. For example, the SEM images of the as-synthesized Zn-added $GdPO_4$:Tb^3 powders with Zn/Gd = 0.015/0.835 and 0.03/0.82 are shown in Fig. 1(a) and (b), respectively. The added Zn^{2+} and Tb^{3+} had no significant influence on the synthesized powder characteristics.

However, the powder characteristics of the annealed phosphors depended strongly on both the Zn^{2+} content and the annealing temperature. The annealed Zn^{2+}-free $GdPO_4$:Tb^3 phosphors showed high-quality powder characteristics, irrespective of annealing temperature. For example, the SEM images of the Zn^{2+}-free $GdPO_4$:Tb^3 phosphors annealed at 800 and 1000 °C are shown in Fig. 2(a) and (b), respectively. On the other hand, the powder characteristics of the Zn^{2+}-added $GdPO_4$:Tb^3 phosphors depended strongly on both the Zn^{2+} content and the annealing temperature. The powder characteristics of all the Zn^{2+}-added phosphors annealed at 800 °C were nearly equivalent to those of the synthesized phosphors, irrespective of Zn^{2+} content.

The powder characteristics of the Zn^{2+}-added phosphors were gradually deteriorated with increases in the annealing temperature and Zn^{2+} content. At the annealing temperature of 900 °C, the Zn^{2+}-added $GdPO_4$:Tb^3 phosphors with low and medium Zn^{2+} contents (≤0.03) showed high-quality powder characteristics, whereas those with high Zn^{2+} contents (≥0.045) showed less regular, smooth and spherical morphology. For higher annealing temperatures (≥1000 °C), the powder characteristics became worse with increase in the annealing temperature and the Zn^{2+} content. For example, the SEM images of the Zn^{2+}-added $GdPO_4$:Tb^3 phosphors with Zn/Gd = 0.015/0.835 and 0.03/0.82 annealed at 900 and 1000 °C are shown in Fig. 3(a) and (b), respectively.

Fig. 4(a) and (b) reveals the XRD patterns of the phosphors annealed at 800 and 900 °C, respectively. All the phosphors annealed at 800 °C crystallized in a solid solution of constituent oxides with the monoclinic monazite structure [14]. In addition, at the annealing temperature of 900 °C, the $GdPO_4$:Tb^3 phosphors with low and medium Zn^{2+} contents (≤0.03) formed a solid solution of constituent oxides with a monoclinic monazite structure. On the other hand, in addition to the solid solution, the $GdPO_4$:Tb^3 phosphors with high Zn^{2+} contents ($x \geq 0.045$) contained a secondary phase $Zn_3(PO_4)_2$ [15]. The amount of $Zn_3(PO_4)_2$ became more pronounced with increasing Zn^{2+} content. The crystal structure of the $GdPO_4$:Tb^3 phosphors annealed at 1000 and 1100 °C was basically equivalent to that at 900 °C.

Table 1
Calculated crystallite size of the annealed $GdPO_4$:Tb^3 phosphors with various Zn^{2+} contents as a function of annealing temperature.

Sample	Annealing temperature (°C)	Crystallite size (nm)
$GdPO_4$:Tb^3 with Zn/Gd = 0/0.85	800	27.9
	900	31.6
	1000	33.3
	1100	40.5
$GdPO_4$:Tb^3 with Zn/Gd = 0.015/0.835	800	29.5
	900	34.7
	1000	35.4
	1100	41.7
$GdPO_4$:Tb^3 with Zn/Gd = 0.03/0.82	800	29.8
	900	37.3
	1000	38.8
	1100	54.3
$GdPO_4$:Tb^3 with Zn/Gd = 0.045/0.805	800	29.9
	900	53.5
	1000	55.8
	1100	58.2
$GdPO_4$:Tb^3 with Zn/Gd = 0.06/0.79	800	30.6
	900	49.5
	1000	53.8
	1100	53.9

The crystallite size (D) of the annealed phosphors was calculated from the Scherrer formula: [16] $D = (0.9\lambda)/(\beta \cos\theta)$, where λ is the wavelength of radiation, θ is the angle of the diffraction peak, and β is the full width at half maximum of the diffraction peak (in radian). The calculated crystallite size of the annealed phosphors as functions of annealing temperature and Zn^{2+} content is given in Table 1. The crystallite sizes increased with increase in the annealing tem-

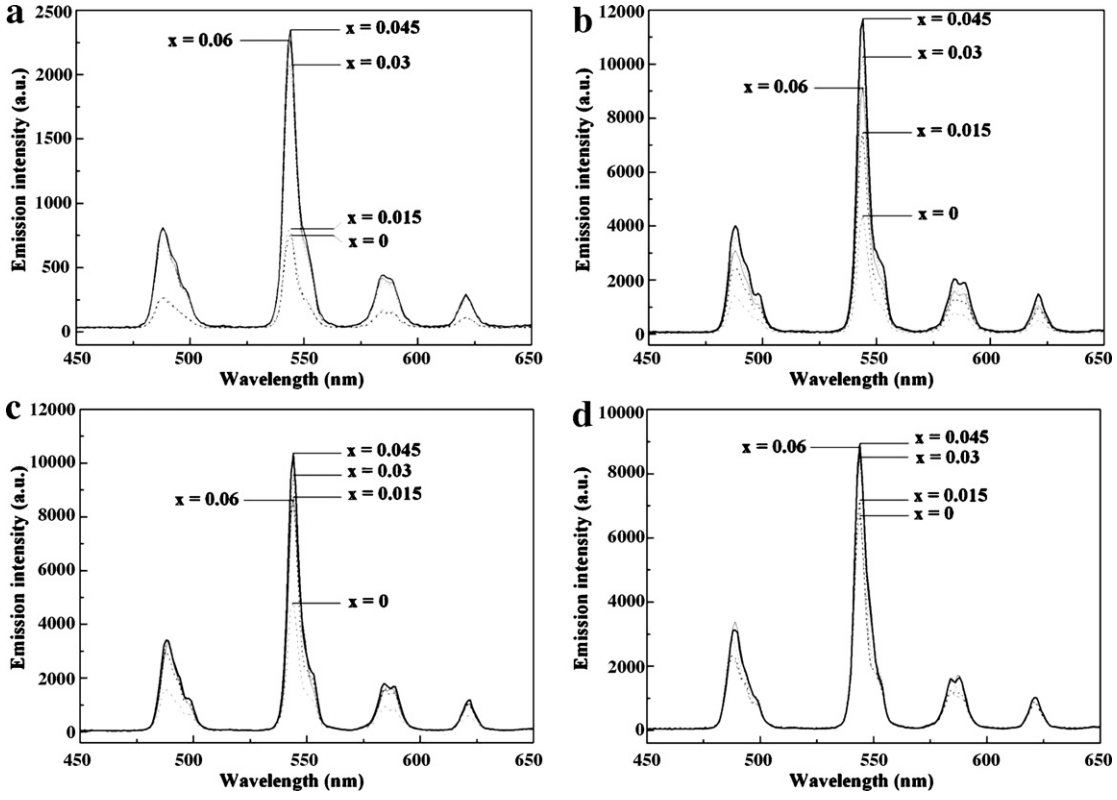

Fig. 5. Emission spectra of the $GdPO_4$:Tb^3 phosphors with various Zn^{2+} contents annealed at (a) 800 °C, (b) 900 °C, (c) 1000 °C, and (d) 1100 °C.

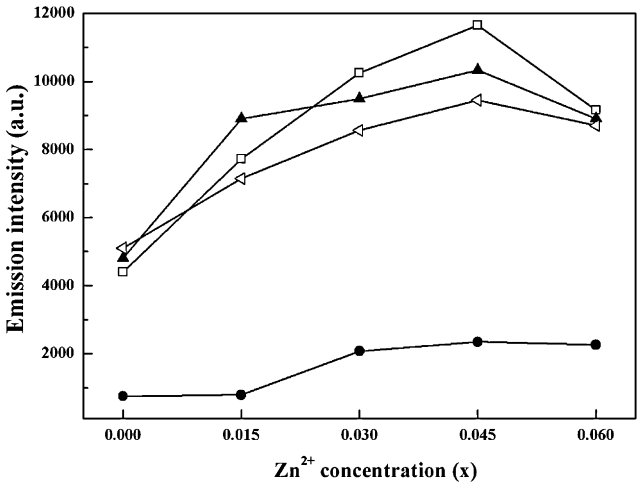

Fig. 6. Emission intensity of the $GdPO_4$:Tb^3 phosphors with various Zn^{2+} contents at 544 nm under VUV excitation as a function of annealing temperature (●: 800 °C; □: 900 °C; ▲: 1000 °C; and ◁: 1100 °C).

perature and the Zn^{2+} content except for the Zn-added $GdPO_4$:Tb^3 with Zn/Gd = 0.06/0.79.

From the viewpoint of practical applications in PDPs, the emission spectra of the Zn-added $GdPO_4$:Tb^3 phosphors annealed at various temperatures (800–1100 °C) were obtained under VUV excitation (147 nm), along with the Zn-free phosphors. The emission spectra of the Zn-free and added $GdPO_4$:Tb^3 phosphors annealed at 800–1100 °C are shown in Fig. 5. The main emission peaks are located at 489, 544, 585, and 621 nm which are caused by the $^5D_4$–^7F_J (J = 6, 5, 4, and 3) transitions of Tb^{3+}, respectively [17]. The peak corresponding to the $^5D_4$–$^7F_5$ transition, which is responsible for the green emission, is dominant among the emission peaks.

The emission intensity of the Zn-free and added $GdPO_4$:Tb^3 phosphors at 544 nm under VUV excitation is summarized in Fig. 6, depending on the annealing temperature and the Zn^{2+} content. For the Zn-free $GdPO_4$:Tb^3 phosphors, the emission intensity increased with the annealing temperature. The increased intensity is caused by a larger crystallite size [18]. A large crystallite size provides higher oscillating strengths for the optical transitions due to the improved crystallinity, increased interaction area with the excitation light, and reduced loss [18–21]. For a low Zn^{2+} content (0.015), the strongest emission was obtained for the phosphors annealed at 1000 °C. This occurred primarily because their crystallite size was larger, compared to the phosphors annealed at 800 and 900 °C, and their morphology was smooth and spherical. Although the phosphors annealed at 1100 °C had the largest crystallite size, they had poor powder characteristics, e.g., rough and non-spherical morphologies. In addition, for higher Zn^{2+} contents (≥0.03), the phosphors annealed at 900 °C showed the most intense emission. This is due to the fact that the phosphors annealed at higher temperatures (≥1000 °C) had poor powder characteristics.

The emission intensities at 544 nm for the Zn^{2+}-added $GdPO_4$:Tb^3 phosphors with Zn/Gd = 0.015/0.835, 0.03/0.82, 0.045/0.805, and 0.06/0.79 annealed at 900 °C were 176, 233, 265, and 208% stronger, respectively, in comparison with the Zn^{2+}-free $GdPO_4$:Tb^3 phosphors annealed at 900 °C. This means that the addition of Zn^{2+} for Gd^{3+} is highly favorable for improving the PL properties. In addition, at a fixed Zn^{2+} content of 0.045, the emission intensities at 544 nm for the phosphors annealed at 900, 1000, and 1100 °C were 496, 440, and 275% stronger than that at 800 °C, respectively. Based on the above results, for fabricating high-efficiency Zn^{2+} added $GdPO_4$:Tb^3 phosphors, it is necessary to control the Zn^{2+} content, the annealing temperature, the crystallite size, and the powder characteristics.

4. Conclusions

We synthesized high-quality Zn-free and added $GdPO_4$:Tb^3 green phosphors, i.e., fine size as well as smooth and spherical morphologies, by ultrasonic spray pyrolysis. The phosphors annealed at 800 °C maintained their synthesized powder characteristics and were solid solutions of the constituent oxides with the monoclinic monazite structure. The higher annealing temperature (900–1100 °C) led to less smooth, regular, and spherical morphologies. In addition, the crystal structure of the phosphors annealed at 900–1100 °C was strongly dependent on the Zn^{2+} content. The $GdPO_4$:Tb^3 phosphors with low and medium Zn^{2+} contents (≤0.03) were a single phase with the monoclinic monazite, and those with high Zn^{2+} contents (≥0.045) consisted of a solid solution of constituent oxides and a secondary phase $Zn_3(PO_4)_2$.

The emission intensity of the Zn added $GdPO_4$:Tb^3 phosphors depended strongly on the Zn^{2+} content and the annealing temperature. The emission intensity of the phosphors at 544 nm increased with an increase in Zn^{2+} content up to 0.045 and then decreased for higher Zn^{2+} content. The emission intensities at 544 nm for the Zn^{2+} added $GdPO_4$:Tb^3 phosphors with Zn/Gd = 0.045/0.805 annealed at 900, 1000, and 1100 °C were 496, 440, and 275% stronger than that at 800 °C, respectively. For the Zn^{2+} added $GdPO_4$:Tb^3 phosphors, the magnitude of the emission intensity depended strongly on the annealing temperature and followed the order of 900 > 1000 > 1100 > 800 °C.

References

[1] C. Feldmann, T. Jüstel, C.R. Ronda, P.J. Schmidt, Adv. Funct. Mater. 13 (2003) 511–516.
[2] B. Yan, X. Su, Opt. Mater. 29 (2007) 1866–1870.
[3] V. Natarajan, A.R. Dhobale, C.H. Lu, J. Lumin. 129 (2009) 290–293.
[4] J. Lin, G. Yao, Y. Dong, B. Park, M. Su, J. Alloys Compd. 225 (1995) 124–128.
[5] S. Erdei, F.W. Ainger, D. Ravichandran, W.B. White, L.E. Cross, Mater. Lett. 30 (1997) 389–393.
[6] M. Heike, R. Karsten, K. Andrew, N. Sabine, H. Markus, Adv. Mater. 11 (1999) 840–844.
[7] B. Finke, L. Schwarz, P. Gürtler, M. Kraas, M. Joppien, J. Becker, J. Lumin. 60–61 (1994) 975–978.
[8] R.P. Rao, D.J. Devine, J. Lumin 87–89 (2000) 1260–1263.
[9] W. Di, X. Wang, B. Chen, H. Lai, X. Zhao, Opt. Mater. 27 (2005) 1386–1390.
[10] H. Dong, Y. Liu, P. Yang, W. Wang, J. Lin, Solid State Sciences 12 (2010) 1652–1660.
[11] N. Niu, P. Yang, Y. Wang, W. Wang, F. He, S. Gai, D. Wang, J. Alloys Compd. 509 (2011) 3096–3102.
[12] K. Park, J.K. Lee, Y. Kwon, S.-J. Kim, S. Nahm, J. Nanosci. Nanotechnol. 8 (10) (2008) 5503–5505.
[13] J.H. Lee, M.H. Heo, S.-J. Kim, S. Nahm, K. Park, J. Alloys Compd. 473 (2009) 272–274.
[14] JCPDS file No. 26-0660.
[15] JCPDS file No. 76-0604.
[16] B.D. Cullity, Elements of X-ray Diffraction , Addison-Wesley, Reading, MA, 1978.
[17] C.K. Lin, M.L. Pang, M. Yu, J. Lin, J. Lumin. 114 (3–4) (2005) 299–306.
[18] K.S. Shim, H.K. Yang, B.K. Moon, B.C. Choi, J.H. Jeong, J.H. Kim, J.S. Bae, K.H. Kim, Curr. Appl. Phys. 9 (2009) S226–S229.
[19] K.C. Misbra, J.K. Berkowitz, K.H. Johnson, P.C. Schmidt, Phys. Rev. B 45 (1992) 10902–10906.
[20] J. Szczyrbowski, A. Czapla, Thin Solid Films 46 (1977) 127–137.
[21] S.L. Jones, D. Kumar, R.K. Singh, P.H. Holloway, Appl. Phys. Lett. 71 (1997) 404–406.